Aeroelastic and Biodynamic Modelling for Stability Analysis of Rotorcraft-Pilot Coupling Phenomena

J. Serafini, M. Gennaretti
University Roma Tre
m.gennaretti@uniroma3.it, serafini@uniroma3.it

P. Masarati, G. Quaranta
Politecnico di Milano
pierangelo.masarati@polimi.it, giuseppe.quaranta@polimi.it

O. Dieterich
Eurocopter Deutschland GmbH
oliver.dieterich@eurocopter.com

Keywords: Rotorcraft-Pilot Coupling, Aeroservoelasticity, Pilot Biomechanics, Vertical Bouncing.

Abstract

This paper presents the current status of the investigation conducted by the authors as part of the GARTEUR HC AG-16 on Rotorcraft-Pilot Couplings (RPCs) governed by aeroservoelastic interactions. Phenomena of this type are caused by an 'abnormal' interaction between the pilot biodynamics and the rotorcraft structural dynamic response, and usually take place in the frequency range from 2 to 8 Hz. Complex multidisciplinary numerical models must be developed to accurately reproduce the mechanism that leads to this type of instability. To broaden the limited amount of information available in the open literature on rotorcraft pilot's biodynamic response, a specific test campaign has been performed. The main results of these tests are presented in the paper. Original rotorcraft and pilot models developed by the authors, complemented by models taken from the literature, are used for the analysis of complete helicopter configurations, to single out possible occurrences of aeroelastic RPCs and analyse their sensitivity to several parameters.

1 Introduction

This paper presents the current status and the results of part of the research activity performed in the framework of the GARTEUR HC AG-16 on Rotorcraft-Pilot Coupling (RPC) [1]. An overview of the overall activity of Action Group 16 is presented in [2], while a detailed description of the experimental test campaigns and of the rigid body RPC investigation is given in the companion papers [3] and [4], respectively. The paper deals with what has been defined 'aeroelastic' RPCs (see [2]), i.e. adverse interactions that cause the appearance of sustained oscillations in the frequency range from 2 to 8 Hz. These phenomena may represent a potential threat for the airworthiness of rotorcraft. The occurrence of this kind of events is not well documented in the open literature. An interesting survey of aeroelastic RPCs, mainly for US Navy and Marine Corps rotorcraft, can be found in Ref. [5].

The mechanism that may cause the instability is quite clear and is usually called Pilot Assisted Oscillations (PAO) [5]: the pilot, while seating in the cockpit, is subjected to vibrations transmitted through the elastic airframe. When the frequencies of these vibrations are above 2 Hz, they are not reacted by the pilot, who may eventually perceive them as annoying, if he/she perceives them at all [6]. As a consequence, these oscillations are transmitted to the aircraft control sticks, introducing

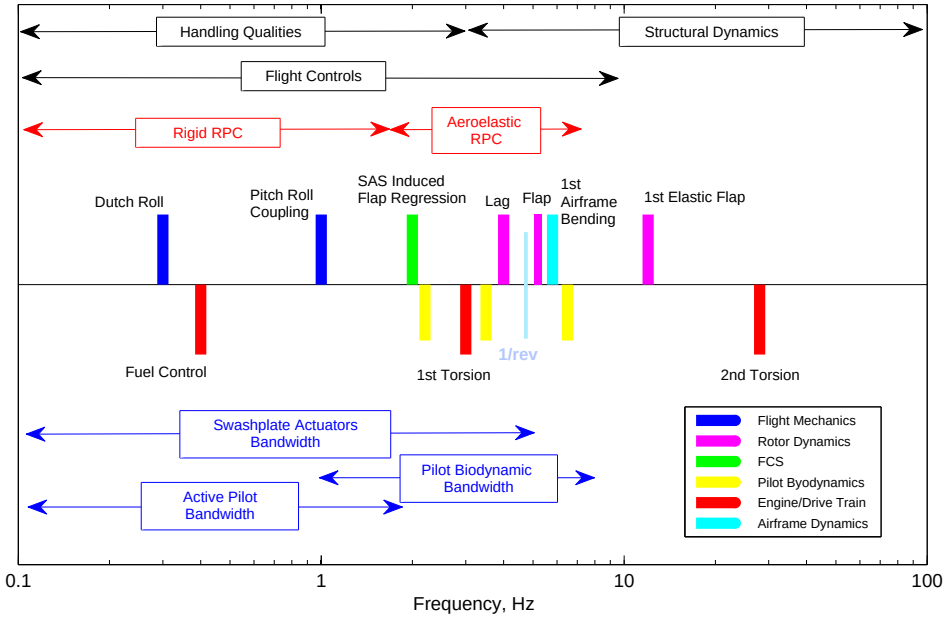

Figure 1: Frequency range characteristic of rotorcraft dynamics.

an unintentional high frequency[1] control action that may lead to the sustained oscillations. The ratio between the airframe vibration input and the signal introduced into the control sticks is ruled by the pilot's biodynamic impedance, which is called throughout this work the *passive pilot* model, to emphasise the fact that the pilot acts on the controls in a way that is independent from his/her will.

Figure 1 sketches the location of the characteristic frequencies of interest in rotorcraft, classified in terms of the different system components they belong to. Numerous elements that can interact are interested by the range of frequencies affected by aeroelastic RPCs: rotor dynamics, airframe dynamics, Flight Control System (FCS), drive train dynamics and, of course, pilot biodynamics. Additionally, the swashplate actuators may play a significant role, since their bandwidth usually falls somewhere in this range, possibly causing significant interactions with the other players of this tangled instability mechanism. As a consequence, the complexity and the level of detail required to predict this type of events is very high, suggesting the adoption of comprehensive aeroservoelastic models developed *ad hoc* for this purpose. Figure 2 shows a block diagram that illustrates all the required elements, along with their interconnections. The capability to model aeroelastic RPCs is strongly related to the ability to model the coupled rotor aerodynamics, the structural dynamic behaviour of each single part of the rotorcraft including the pilot, and the possible interactions with the external environment. In fact, as clearly reported in the literature [7, 5], the appearance of a PAO event is often caused by a change in some of the elements participating in the dynamics, triggered by a change in the operating environment or in the Mission Task Element (MTE). In fact, this change is often referred to as the *trigger* of the instability event.

This paper presents the analysis of pilot-rotorcraft aeroelastic interaction performed by University Roma Tre (UROMATRE), Politecnico di Milano (POLIMI) and Eurocopter Deutschland GmbH (ECD). Among the different PAO mechanisms, the focus has been placed on the vertical bouncing, a type of instability that may arise mainly from the coupling between vertical oscillations of the airframe and collective flap rotor dynamics, which is fed back by the pilot's impedance. In fact, for classical rotorcraft control sticks layout, a vibration along the vertical axis may cause the involuntary introduction of collective control input. As a consequence, the collective rotor flapping (cone) dynamics may be excited, eventually resulting in sustained vertical oscillations of the airframe. The

[1]Here 'high frequency' means 'beyond the frequency range pilot control actions could intentionally occur at'.

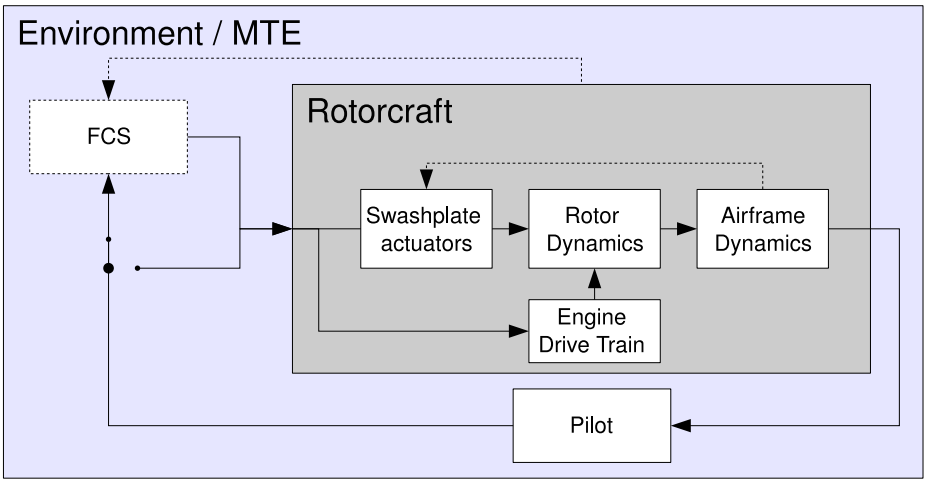

Figure 2: Block diagram of interactions between rotorcraft model elements.

numerical investigation exploits the general availability of the BO105 light helicopter database, although the BO105 is not known to be prone to this type of instability [2]. Both the hover and steady forward flight conditions are considered. The three research groups independently applied different rotorcraft aeroelastic simulation tools to this problem, as shown in Section 2. Only a limited amount of information is available in the open literature for the pilot biodynamics, especially for typical rotorcraft collective configurations. The transfer functions presented in [8] have been used as a starting point. However, this type of transfer functions is strongly linked to the geometric arrangement of the cockpit where the experimental measures are performed. To overcome these limitations, and to gain more confidence in the analysis of the biodynamic behaviour of helicopter pilots, POLIMI performed a preliminary experimental campaign for the characterisation of the biodynamic response, related to the collective stick. The details of the experimental set up for the campaign performed with the flight simulator of the University of Liverpool are presented in [3]. The main results achieved up to now from the analysis of the measured data are presented in Section 3 of this paper. The stability analysis of the coupled pilot-rotorcraft models and the sensitivity of the problem to various aspects, performed by the different research groups, are detailed in Section 4. A final Section is dedicated to the individuation and implementation of possible means of prevention for aeroelastic RPCs.

2 Aeroelastic Modelling

Different characteristic elements of rotorcraft dynamics concur to the onset of aeroelastic RPCs, as shown in Figure 2. One of the objectives of this research consists of determining the level of detail that is needed to detect the instability. For this reason, the Action Group decided to approach rotorcraft modelling using different methodologies for each research group, in order to exploit the different expertise. Table 1 summarises the relevant elements of the modelling approach followed by each research group. A more detailed description is presented in the following paragraphs. The aerodynamics of the main rotor is based for all models on the blade element theory, with the addition of inflow models of different levels of complexity. Steady coefficients depending on pitch and yaw angles are used to compute airframe aerodynamic forces. The main differences are related to the dynamics of the main rotor, which is one of the most critical elements for the vertical bouncing. The three models have been compared in terms of eigenvalues and eigenvectors around several trim points to ensure that a common baseline is shared among the research groups. However, the different approaches allowed to carry out sensitivity analyses in a broad variety of directions, exploiting the capabilities of each specific implementation of the BO105 aeroelastic model. All data required to describe the dynamics of the BO105 are presented in [2].

Table 1: Modelling approaches followed by the research groups.

Group	**ECD**	**POLIMI**	**UROMATRE**
Rotor dynamics	modal	FEM	modal
Rotor aero.	QS + dynamic inflow	QS + uniform inflow	QS + free-wake inflow
Fuselage dynamics	6 linear rigid DOFs + modal elasticity	6 nonlinear rigid DOFs + modal elasticity	6 linear rigid DOFs + modal elasticity
Fuselage aero.	stationary	stationary	stationary
Swashplate	transfer function + hub linear springs	transfer function + multibody hub dyn.	transfer function + hub linear spring
Linear Stability analysis	multiblade eigenvalues	system identification of time series	Floquet eigenvalues

QS: Quasi Steady blade element theory;
FEM: Nonlinear Finite Element Model

2.1 ECD Modelling

The dynamics of the BO105 helicopter are represented using a state space, constant coefficient model derived from the comprehensive rotor and helicopter code CAMRAD II [9] by exporting a linearised system in multi-blade coordinates. The numerical model used for aeroelastic RPC studies was based on an elastic airframe model, an elastic main rotor model and a rigid tail rotor for trim purposes. For the simplified vertical bouncing problem, the interfaces of the helicopter model were reduced to one input and one output leading to a SISO system (Single Input Single Output). The input channel consisted of the main rotor collective control – unit degree blade pitch – while the output could be switched between different airframe grid points related to the vertical acceleration of the elastic airframe. The complete helicopter model consisted of the following 72 states:

- 9 rigid body states of the helicopter (translations: first order; rotations: second order);
- 3 main rotor dynamic inflow states (collective, lateral, longitudinal: all first order);
- typically 6 elastic airframe states: 3 elastic airframe modes;
- typically 8 to 10 states per main rotor blade: 4 to 5 elastic blade modes;

This kind of model allows to perform parametric studies with respect to the most relevant variables for the rotorcraft design: fuselage frequencies, pilot position, structural damping, and so on.

2.2 POLIMI modelling

The model developed at Politecnico di Milano is based on a multidisciplinary multibody modelling approach using the free multibody analysis software MBDyn [10]. This software is mainly intended for the solution of Initial Value Problems (IVP) by direct time integration, typically by using unconditionally stable implicit integration algorithms.

The main rotor is modelled by geometrically nonlinear beam elements based on an original Finite Volume approach, which allows to capture the dynamics of arbitrarily anisotropic rotating beams to the desired level of accuracy. The kinematics and dynamics of the blade root, consisting of a flexbeam and a pitch bearing for each blade, is modelled without simplifications, as well as the pitch control chain. The tail rotor is represented using a simple, rigid blade model. The airframe is modelled by means of Component Mode Synthesis (CMS), using a special element that superimposes the linear combination of deformation shapes to the arbitrary rigid-body dynamics of a node. The dynamics of

the deformation shapes are governed by second-order linear differential equations, exploiting modal analysis results.

A peculiarity of this type of analysis is that it closely resembles an experiment, as trim and stability analysis cannot be decoupled. In fact, the trim is reached in terms of a nearly-steady condition at the end of the integration of a transient with respect to time. For this purpose, an external integral (not necessarily realistic) autopilot has been implemented in Simulink to control the flight of the helicopter up to the desired trim condition. Depending on the type of analysis, if a stable trim point is reached the autopilot can be either left in place or switched off, to assess the stability of the uncontrolled system. The stability of the system is assessed by perturbing the trim condition, and by identifying the response of the system. Conventional system identification techniques can be used; in order to exploit the availability of significant redundancy from the simulation output, a technique based on the Proper Orthogonal Decomposition (POD) has been developed [11].

2.3 UROMATRE modelling

The dynamics of the helicopter fuselage is described through the Newton-Euler equations for the six degrees of freedom related to rigid-body motion. Forcing terms are given by the main and tail rotor loads transmitted at the hubs and by the airloads generated on fuselage, fin and tail plane surfaces. To take into account the effects of the airframe elastic deformation, the rigid-body model described by the nine rigid-body motion state variables (three linear and three angular velocities, plus the three Euler angles) is enriched by including the elastic degrees of freedom associated to the natural vibration modes of the fuselage. A set of equations is added to the system for the dynamics of the elastic fuselage. The elastic deformations combined with the rigid-body motion yield the linear and angular hub displacements that produce perturbations to the inertial and aerodynamic loads on the rotor blades.

The aeroelastic modelling of the main rotor blades is based on the nonlinear flap-lag-torsion equations of motion presented by Hodges and Dowell [12], combined with a 2D quasi-steady aerodynamics derived from Greenberg theory [13]; the equations are spatially integrated through the Galerkin approach. Inflow models for the rotor are given either by an analytical model or by a free-wake analysis based on the boundary integral aerodynamic solver described in [14]. The set of coupled equations governing the motion of the elastic airframe, the dynamics of main rotor blades and the biodynamic pilot behaviour is linearised through an analytical-numerical procedure, about a steady periodic equilibrium state, obtained by a classical trim procedure. Then, the Floquet theory is applied to the resulting set of periodic-coefficient ordinary differential equations in order to perform the eigenvalue stability analysis of the closed loop fuselage/rotor/pilot dynamics.

3 Transfer Function Pilot Modelling

A common approach to the modelling of the pilot's influence on aircraft aeroservoelasticity consists of identifying an equivalent transfer function that relates the motion of the controls in response to the vibratory load the pilot receives from the seat. Single Input-Single Output (SISO) models are often considered, where the motion of a single control is related to a specific component of the acceleration of the seat, to address specific manoeuvres or flight conditions. This approach may be questionable from many points of view, as the effects of different sources of vibration may not be easily separated. However, it provides a useful tool to consider the problem from a simple and effective point of view.

Quite a few examples of experimental transfer functions identified for similar purposes can be found in the literature. In many cases, they address the very low frequency range that is typical of flight mechanics of fixed wing aircraft.

Well-known examples of transfer functions specifically intended for rotorcraft analysis are provided by Mayo in [8] for the collective control, and by Parham *et al.* in [15, 16] for the V–22 longitudinal cyclic control. In this work, the focus is mainly on the collective control.

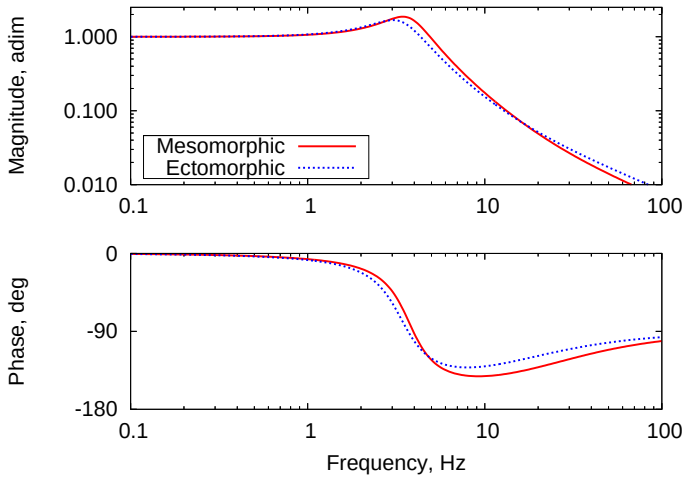

Figure 3: Comparison between 'ectomorphic' and 'mesomorphic' pilot transfer functions (from [8]).

Table 2: Pilot data (from [8]).

	Ectomorphic	**Mesomorphic**
Height	5.9 in (1.75 m)	6.1 in (1.85 m)
Weight	152.0 lb (70 kg)	198.0 lb (90 kg)
Frequency	3.20 Hz	3.60 Hz
Damping	32.2 %	28.2 %

3.1 Collective Control SISO Transfer Function

In [8], two functions are proposed. They have been estimated from measurements obtained for two groups of pilots of different size, called 'ectomorphic' (smaller size),

$$H_{\text{ecto}} = \frac{5.19s + 452.3}{s^2 + 13.70s + 452.3}, \tag{1}$$

and 'mesomorphic' (larger size),

$$H_{\text{meso}} = \frac{4.02s + 555.4}{s^2 + 13.31s + 555.4}. \tag{2}$$

The functions are compared in Figure 3, and their properties are summarised in Table 2. In the original reference the ectomorphic function appeared to be more prone to instability when coupled with the dynamics of a heavy helicopter.

A dependence of the amplification factor on the reference angle of the collective control stick is observed, as illustrated in Figure 4. This is explained with the different configuration of the pilot's arm, which changes from almost entirely extended (low collective settings) to significantly bent (high collective settings). The amount of information provided by the transfer functions of Eqs. (1) and (2) and by Figure 4 is not sufficient to fully understand the pilot dynamics at different reference collective control angular positions, since the change in the attitude of the involved limbs could modify the transfer function not only in terms of amplification factor, but also in terms of poles and zeros, as highlighted in a following section.

The transfer functions of Eqs. (1) and (2) represent the absolute acceleration of the hand holding the collective control stick as a function of the vertical acceleration of the seat. In order to apply it to direct time integration, they have been modified to provide the relative motion of the stick by adding a double pseudo-integrator to the transfer function $H_{\text{rel}}(s) = H(s) - 1$, that represents the relative

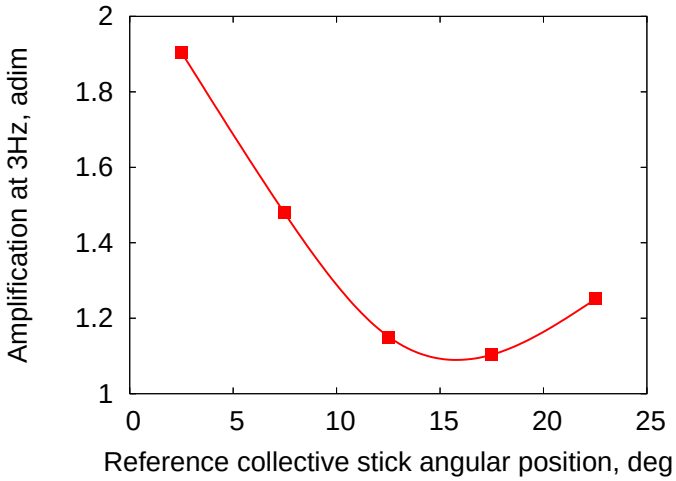

Figure 4: Amplification factor between pilot seat and collective stick angular position when excited at 3Hz, for a single pilot and a reference trim angular position of 11.25 deg (from [8]).

acceleration of the stick. The resulting function is

$$H'_{\text{rel}} = \frac{1}{s}\frac{1}{s+\alpha}\left(H-1\right), \tag{3}$$

where the first integrator $1/s$ cancels the zero in the origin resulting from the $H\left(s\right)-1$ term, while the second has been modified into $1/\left(s+\alpha\right)$, with α corresponding to a very low frequency pole (0.1 Hz in the present case) to eliminate any possible drift. The rationale is that at very low frequencies the pilot can compensate any acceleration that moves its arm, so a static acceleration can only result at most in a static deflection of the control. In any case, the very low frequency behaviour of the pilot is outside the scope of the present work, while it may be of interest for rigid body RPC, discussed in [4].

During AG-16 experimental activity, specific biomechanical tests have been conducted at University of Liverpool [3]. The tests mainly consisted of the vertical harmonic and random excitation of two human subjects, indicated as pilot #1 and #2 in the following, sitting in UoL's flight simulator and grabbing the collective control. The resulting data allowed to identify the corresponding transfer function, in terms of percent of control rotation as a function of the acceleration of the base, in g, for different subjects and different reference collective control settings. The resulting functions seem to be characterised by a 4th order denominator and a 2nd order numerator, respectively made by two pairs of complex conjugated poles and one pair of complex conjugated zeros, namely

$$H' = G\frac{\left(s+z\right)\left(s+z^*\right)}{\left(s+p_1\right)\left(s+p_1^*\right)\left(s+p_2\right)\left(s+p_2^*\right)}, \tag{4}$$

where G is the gain, z is the zero and p_1, p_2 are the poles; the superscript asterisk indicates the complex conjugation. The identified values are reported in Table 3. This function is structurally different from Eq. (3), which is characterised by a 3rd order denominator and a 1st order numerator. The pilot's behaviour appears to be characterised by two frequencies, the lower similar to that presented in [8].

Figure 5 compares the poles of Ref. [8]'s ectomorphic and mesomorphic pilots to pilots #1 and #2 at 10% reference collective control stick position. The figure clearly shows that the lower frequency poles of the pilots identified in this work are closely related to those of [8]. Those poles show a clear dependence on the reference position of the collective control. The higher frequency poles show a less pronounced dependence on the collective, especially in terms of damping. Not only this result confirms the trend indicated by Figure 4 from [8], but also suggests that the behaviour observed in [8] could be related to a substantial modification of the pilot's dynamics.

Table 3: Identified transfer functions properties

Test	Pole #1	Pole #2	Zero	Gain
Pilot #1, 10%	-9.8189 ± 20.4374i	-7.0661 ± 31.2961i	-2.6282 ± 28.3482i	-4465.3
Pilot #1, 50%	-6.6574 ± 19.3086i	-4.9026 ± 35.8785i	-3.5630 ± 27.6716i	-2446.1
Pilot #1, 90%	-4.6876 ± 15.3775i	-3.5824 ± 36.1740i	-7.3902 ± 27.8659i	-1024.9
Pilot #2, 10%	-12.2048 ± 19.8534i	-5.0502 ± 33.7910i	-3.2423 ± 30.9463i	-4431.7
Pilot #2, 50%	-5.9031 ± 16.9689i	-7.7169 ± 38.3072i	-5.7946 ± 24.1660i	-2322.5
Pilot #2, 90%	-1.9331 ± 12.6278i	-6.1569 ± 37.2060i	-6.5938 ± 18.3922i	-1189.0

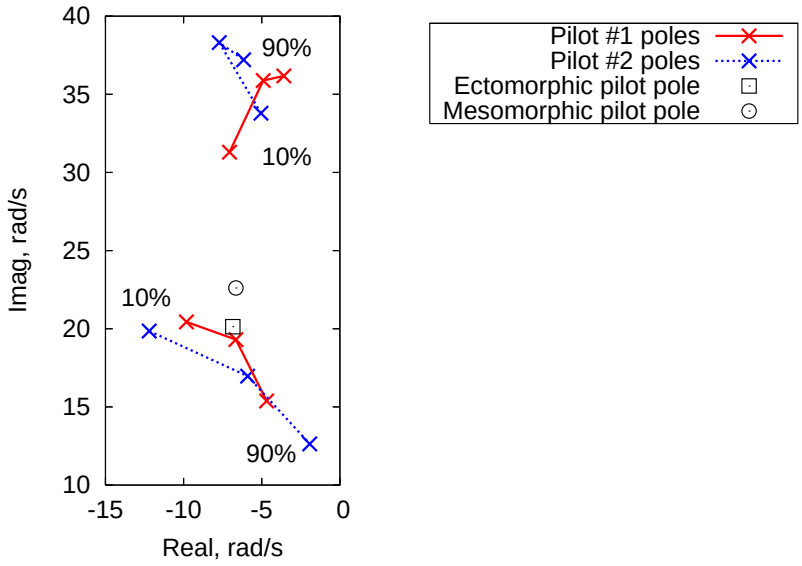

Figure 5: Portion of root locus illustrating the poles of the different pilot models.

The results of the biomechanical investigations suggested the opportunity of developing a generic biodynamic pilot arm model, based on multibody modelling. This model is expected to describe the biodynamic response for a generic configuration of the pilot's limbs. An activity in this direction has been initiated within AG-16. As of this writing, only partial results have been obtained, presented in [17]. This field of research appears definitely promising, and will be further pursued.

3.2 Cyclic Controls SISO Transfer Function

The pilot biomechanical model related to the cyclic controls has been implemented using the transfer functions of Eqs. (5) and (6),

$$H_{\text{lateral}} = \frac{9.4487\text{e+}03\ s\ \text{-}2.8526\text{e+}05}{s^3 + 1.2641\text{e+}03\ s^2 + 9.7102\text{e+}03\ s + 3.8554\text{e+}05} \tag{5}$$

and

$$H_{\text{longitudinal}} = \frac{-9.0227\text{e+}03\ s^2 + 1.4602\text{e+}04\ s + 5.7467\text{e+}07}{s^4 + 1.3085\text{e+}03\ s^3 + 7.5206\text{e+}04\ s^2 + 1.2590\text{e+}07\ s + 3.0382\text{e+}07}, \tag{6}$$

whose Bode plot is presented in Figure 6. They are respectively related to the longitudinal and lateral cyclic control displacement as a function of longitudinal and lateral seat acceleration. The transfer functions of Eqs. (5) and (6) have been identified from data presented in [15], consisting in in/g.

The transfer functions that respectively model the effect of longitudinal and lateral acceleration on the cyclic controls input have been used to separately investigate the effect of each control on the stability of the system. Together with the transfer function that models the effect of the vertical

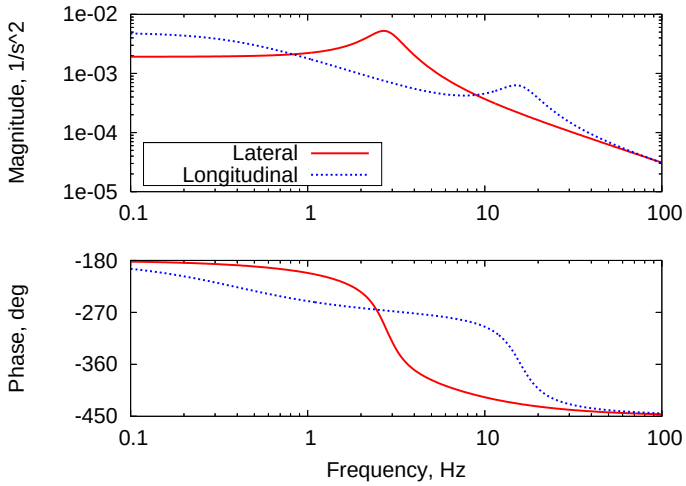

Figure 6: Lateral and longitudinal cyclic transfer functions, describing the displacement of the hand as a function of the acceleration of the seat in the corresponding direction.

acceleration on the collective control input, they have also been used to assess any combined effect resulting from their simultaneous presence. This latter model has been called MIMO, since it simultaneously takes into account the outputs corresponding to multiple input accelerations. However, each acceleration component only acts on one control, so a better denomination would be 'multiple SISO' (MSISO). The term MIMO rather indicates a truly coupled pilot model, capable of describing the combined effect that each acceleration component has on all control inputs in form of a matrix of transfer functions. A model of this sort is not realistically foreseeable with the data available at the time of this writing, but represents a possible, definitely worth pursuing direction for further investigation.

4 Aeroelastic RPCs

For light helicopters, a phenomenon called vertical bouncing is known to be of certain significance in the real world, describing the interaction of the collective control loop with vertical accelerations.

The helicopter model consists of a system featuring collective control as input and pilot and co-pilot seat vertical acceleration as output. This model is connected in feedback with the pilot collective stick biodynamic response. The full scale BO105 is not known to show vertical bouncing, but as a numerical exercise the research group decided to see whether the model could be artificially 'triggered' into a vertical bouncing condition. For this reason a variable gain block is introduced after the pilot transfer function, to represent a generic change in feedback dynamics, which may be caused by a FCS, or other modifications of the pilot transfer function. In fact, by increasing the gain from zero (i.e. no feedback) to one, it can be clearly seen that the poles related to the pilot model cross the imaginary axis, destabilising the system as expected (see the companion paper [2]).

In summary, the analysis of the simplified vertical bouncing problem yields the following results for unit gain:

Ectomorphic pilot: very little damped poles for hover were obtained in the vicinity of the hover stability boundary. Stability increased for increasing flight speeds; nevertheless, an instability was detected at higher speeds.

Mesomorphic pilot: the closed loop configuration seems to be generally more unstable than that of the ectomorphic pilot. Furthermore, the root locus signatures were different with respect to coupling with the ectomorphic pilot.

Ectomorphic co-pilot: An unstable pilot-in-the-loop configuration was detected in hover. In contrast, the closed loop system proved to be stable for the high speed regime represented by the 150

KTAS case.

Mesomorphic co-pilot: Again, an unstable configuration was observed in hover conditions. In the high speed regime of 150 KTAS, the lowest poles of the closed loop system were located in the vicinity of the stability boundary.

5 Sensitivity Analysis

The Action Group decide to perform several sensitivity analysis to gain additional confidence with aeroelastic RPCs and to deepen the knowledge of the parameters that are most influential in the onset of the instability. Each partner focused on different aspects trying to exploited the advantages given by each specific formulation of the rotorcraft dynamic model. Since the main object is the investigation of the closed loop system stability, numerical results show are focused on the behaviour of the real part of system poles, denominated here 'damping' and expressed in 1/s. When the damping goes from negative to positive values, the system goes unstable. As a consequence, on root loci the instability is characterised by the damping crossing the imaginary axis from the left to the right.

5.1 Sensitivity to Structural Modelling Order

Two different parametric studies were performed in order to single out the number of elastic blade and fuselage modes suitable for RPC analysis. Due to the inherent low pass behaviour of the pilot biodynamic impedance, a minor influence of high frequency rotorcraft modes is expected on the stability analysis. However, this is not completely true. Figure 7 shows the behaviour of the least damped eigenvalue of the coupled rotorcraft-pilot system for different choices of rotor blade modes. Results have been obtained for the coupled rotorcraft-pilot system, with feedback gain equal to one, in hover, using Mayo's meso- and ectomorphic transfer functions. The system converges in all cases when all modes up to the first torsion are included. So, even if the blade torsional mode has a frequency close to 25 Hz (see [2]), thus well outside the pilot's biodynamic bandwidth, its static participation to the response seems to have a significant influence on the phenomenon. Similar results were obtained in the high speed case at 150 KTAS level flight, with a slight additional effect of the second lag mode. Figure 8 shows the effect of the rotor blade DOFs on the coupled system poles in hover, confirming the same trend of Figure 7. Note that the FEM blade model used by POLIMI, with

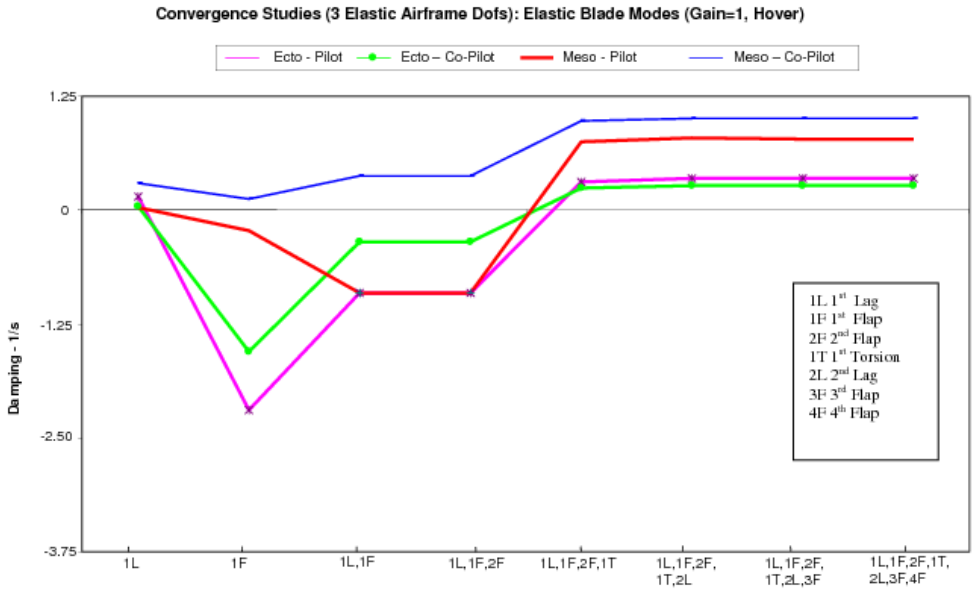

Figure 7: Critical damping levels for different main rotor aeroelastic models in hover.

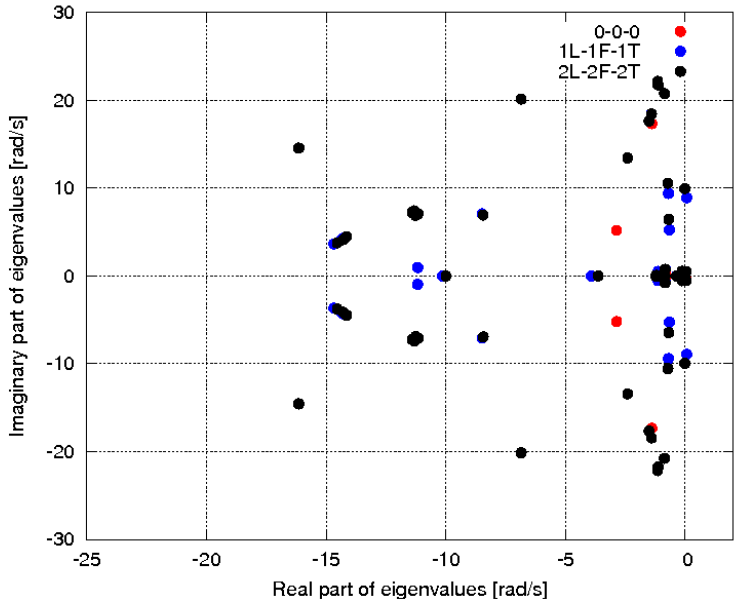

Figure 8: Coupled system poles for different main rotor aeroelastic models in hover.

5 three-node beam elements per blade, and thus 10 nodes per blade, provides an adequate description of the blade modes that guarantee convergence according to Figure 7.

A similar analysis was made to assess the effects of the airframe elastic modes. Figure 9, shows the behaviour of the least damped eigenvalue of the coupled rotorcraft-pilot system for an increasing number of airframe modes. These results suggest the opportunity to select at least three elastic airframe modes for nearly converged results. Only minor changes are observed by including higher airframe modes. Similar results were obtained for the high speed case at 150 KTAS level flight. Figure 10 shows a comparison between linearization about null condition (red dots) and about

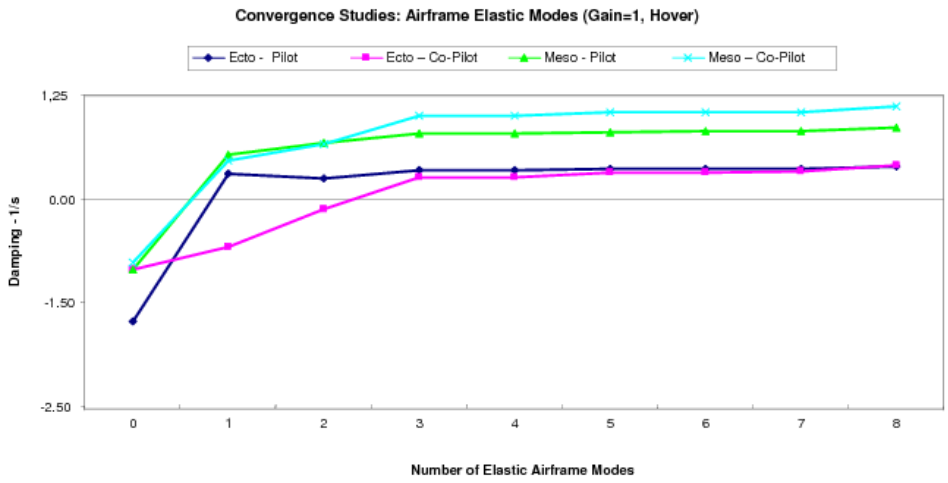

Figure 9: Critical damping levels for different elastic airframe models in hover.

trimmed condition (blue dots). So it seems, at least in hover, that the poles are only slightly affected by non-linear terms.

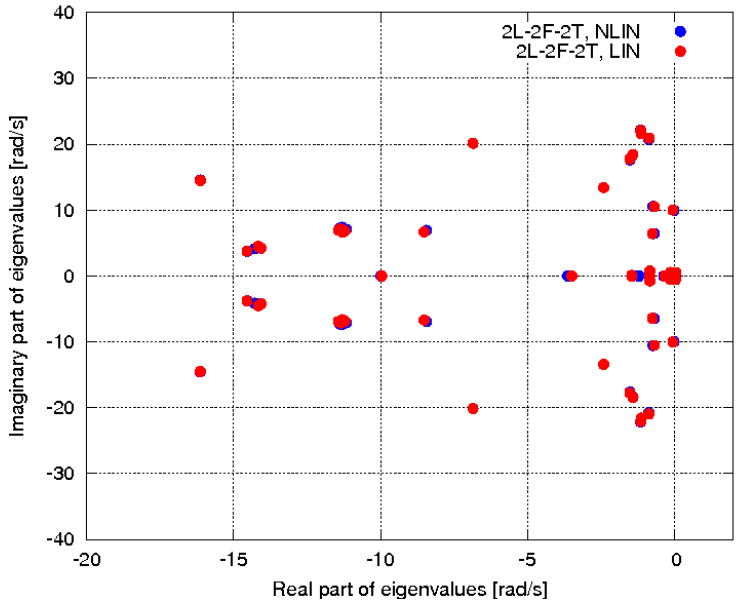

Figure 10: comparison between linearization about null condition and about trimmed condition.

5.2 Sensitivity to Airframe Modal Parameters

ECD performed an investigation of the sensitivity of the stability margins to airframe modal parameters; significantly damping, frequency and modal mass. Due to the significant uncertainty on damping data, and due to the expected impact on the stability of the coupled system, the studies started with modal damping variations for the first elastic airframe mode. The analysed damping values range from 0 to 20% structural damping (corresponding to 10% critical damping). It is worth noticing that the baseline values for all airframe modes consisted of 2% structural damping. While the co-pilot

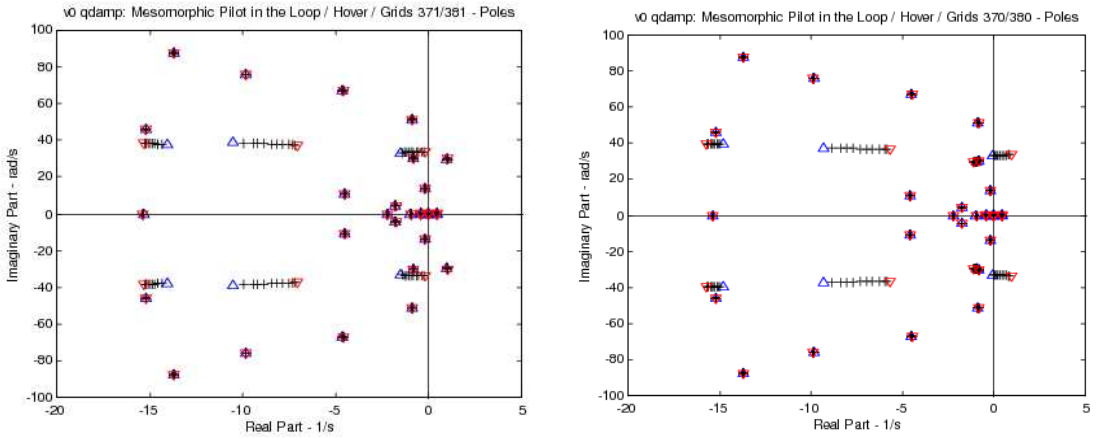

(a) Pilot (b) Co-pilot

Figure 11: Root locus for variation of modal damping of elastic airframe; mesomorphic pilot in hover. ▽ 0%; △ 20%.

position can change from an unstable to a stable configuration by increasing the structural damping, this is not possible for the pilot, whose unstable roots are not affected by an increase in structural damping.

Subsequently, the frequency of the first elastic airframe mode was modified. Two frequency sweeps in different directions were performed starting from the baseline value of 5.8 Hz, ranging from 10 Hz upward to 1 Hz downward. In general, a moderate reduction of the first mode frequency

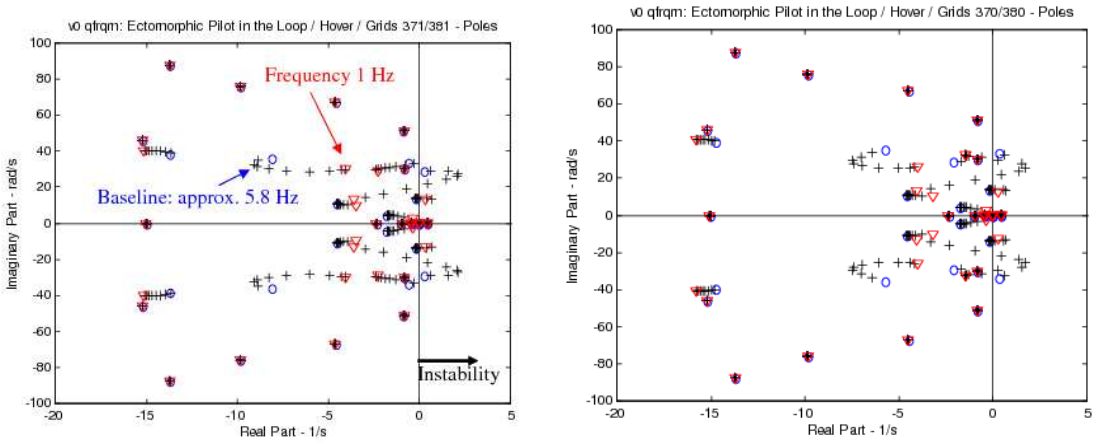

(a) Pilot (b) Co-pilot

Figure 12: Root locus for variation of frequency of first elastic airframe mode; ectomorphic pilot in hover. ○ 10 Hz; △ 1 Hz.

leads to destabilisation. The highest level of instability is reached in the vicinity of 4 Hz. Note, however, that large variations in modal frequencies would probably be accompanied by modifications in the mode shapes. This aspect cannot be taken into account by a simplified sensitivity analysis.

5.3 Sensitivity to Inflow Modelling

During the GARTEUR project, the Roma Tre team focused its attention on the impact of different aerodynamic models in the aeroelastic loop. Due to the embryonic state-of-art in this sense, this research activity aimed at comparing the effects of different inflow models to improve the 2D quasi-steady aerodynamics. In detail, the impact of shed and trailed vorticity on sectional loads were investigated, using different approaches. The shed vorticity due to the unsteady motion of a profile

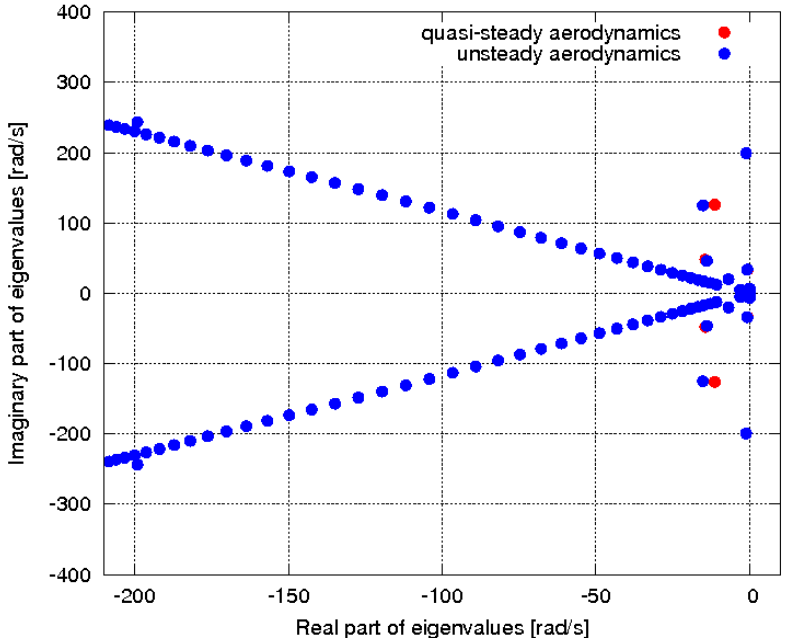

Figure 13: Influence of 2D unsteady aerodynamics on root locus (hover).

in a pulsating flow was included in the model by means of the classical Theodorsen and Greenberg

theories [18, 13], overcoming the hypothesis of low reduced frequencies k implied in the quasi-steady approach. The Theodorsen sectional lift deficiency function was approximated by a two second order polynomial ratio, adding $2 \times N_{\text{section}}$ state variables to the model. A modal expansion of the aerodynamic states using Legendre polynomials was performed along the blade, thus halving the additional states. Figure 13 shows how 2D unsteady effects, while significantly increasing the dimension of the problem, are not so influential (at least for the examined cases) for RPC analysis, since the response of Mayo's pilot model is already negligible at 7–8 Hz, where unsteady effects become significant.

Concerning 3D effects (i.e. trailed vorticity), the inclusion of static inflow models was tested, in order to correct the velocity component normal to the blade. The periodic induced velocity has been computed using a 3D unsteady solver based on the formulation described in [14]. As shown in Figure 14, 3D effects cause an appreciable shift of the poles, including the critical ones, making the introduction of this sophisticated inflow model at least desirable. This represents a first step toward the full inclusion of interactional aerodynamics for RPC analysis, since it involves low frequency phenomena like the ones dominating the interaction between main rotor and tail rotor.

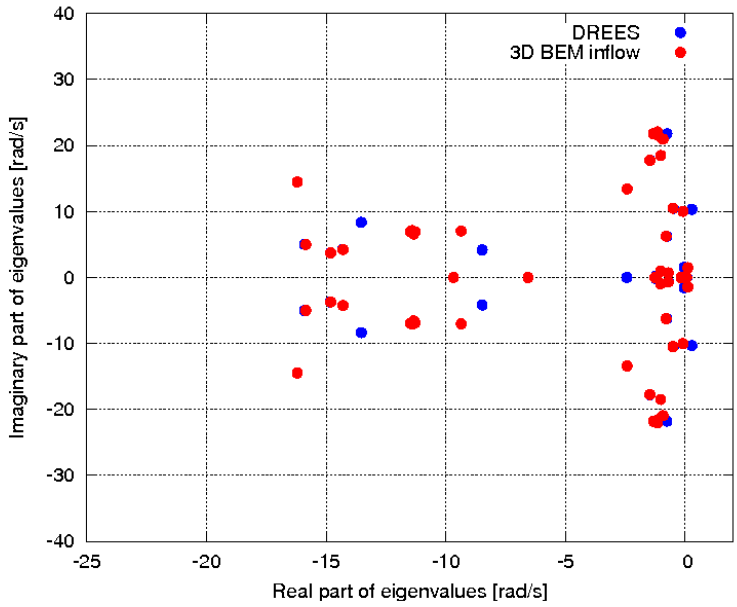

Figure 14: Influence of two different inflow models on root locus (65 KTAS).

5.4 Sensitivity to Swashplate Actuators Dynamics

The modelling of the control system dynamics has been detailed by considering different models of the swashplate actuators' dynamics. In detail, according to available data for the BO105, two very approximate models of the hydraulic actuators dynamics have been considered. In ECD's and UROMATRE's comprehensive models, the dynamics of the actuators are put in series with each pilot's control, namely the collective ($x = 0$) and the two cyclic ($x = c, s$) signals. In POLIMI's multibody model, each actuator is modelled as a separate dynamic subsystem, and receives in input the appropriate combination of collective and longitudinal/lateral cyclic controls. The rotating portion of the swashplate takes care of distributing the appropriate amount of blade pitch input as a function of the azimuthal position of the blade.

In the first case, a 1st order dynamic system has been considered, resulting in the relationship

$$\theta_{\text{out},x} = \frac{\omega_0}{s + \omega_0} \theta_{\text{in},x}, \tag{7}$$

with $x = 0, c, s$ and a characteristic frequency of $\omega_0 = 25$ radian/s, respectively. In the second case,

a 2nd order system was considered, resulting in

$$\theta_{\text{out},x} = \frac{\omega_0^2}{s^2 + 2\xi\omega_0 s + \omega_0^2}\theta_{\text{in},x}, \tag{8}$$

with a damping factor $\xi = 0.4$ and a characteristic frequency of $\omega_0 = 80$ radian/s.

The 1st order actuator model of Eq. (7) showed a stabilising behaviour, while the 2nd order actuator model of Eq. (8) generally resulted in an adverse coupling of the pilot with the dynamics of the rotorcraft. This result is interlocutory and seems to indicate some dependence of the coupled stability of the rotorcraft-pilot system on the control system dynamics. Further investigation of the control system dynamics is required for a better insight into this issue, in view of possible interactions with the FCS in augmented rotorcraft designs.

5.5 Comparison Between Pilot Collective Transfer Functions

The behaviour of the BO105 model in hover has been assessed with respect to different transfer functions of the pilot connected to the collective control stick, when vertical bouncing is considered. The behaviour of the pilot models identified in this project is compared to that of the mesomorphic pilot from [8]. Data corresponding to Pilot #1 at 10% collective setting, according to Table 3, is considered.

The pilot appears to significantly couple with the airframe, similarly to what is experienced when using the pilot models from [8]. The poles directly related to the pilot change, and a significant damping reduction is observed. The transfer functions of Eq. (3) and (4) have been obtained from different types of measurements, and for different cockpit and collective control stick layouts, so a direct comparison is not straightforward.

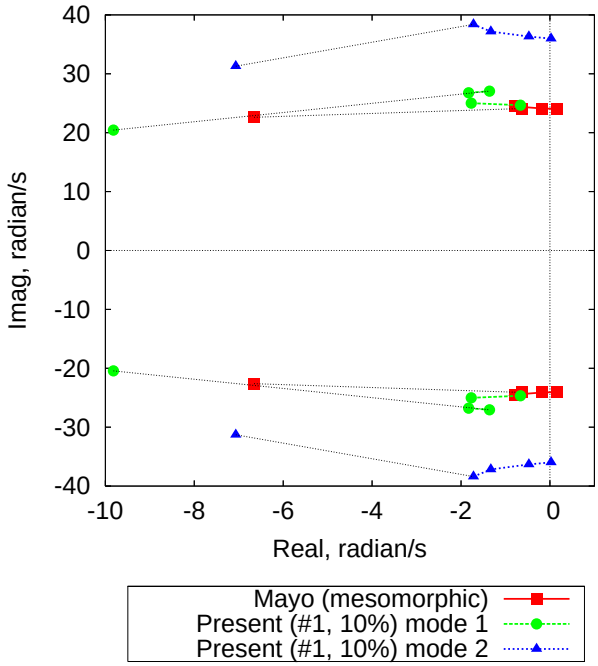

Figure 15: Coupled rotorcraft-pilot root locus of the pilot's poles.

Figure 15 shows that an instability is found for Ref. [8] pilot's root after the pilot's gain is increased. It also shows that when the transfer function of Eq. (4) is used, both the poles it is characterised by show a significant coupling with the rotorcraft dynamics. In detail, it is the higher one that becomes unstable first when the gain is increased.

5.6 Cyclic Pilot Modelling

The impact of the cyclic pilot on the overall rotorcraft stability has been assessed by comparing the open-loop stability of the linearised rotorcraft model with that of the system resulting from separately closing the loop with the pilot transfer functions for the longitudinal and lateral cyclic controls discussed in Section 3.2. Only a minor destabilising effect has been reported, even when the simultaneous effect of the two transfer functions related to the cyclic controls and of the one related to the collective are used, in the so-called MSISO layout. This result is in line with expectations, since there is no direct relationship between any cyclic control and any force in the corresponding lateral direction. As a consequence, no significant dynamic magnification of the pilot's cyclic input can occur.

6 Means of Prevention

The understanding of the nature and cause of aeroelastic RPC finds its practical usefulness in determining possible means of prevention, or at least attenuation, of the phenomenon. The activity performed so far within the AG-16 project with respect to identifying possible cures to aeroelastic RPC mainly consisted of checking the appropriateness of known, common practise approaches, and in outlining lines for possible future research in the field.

Two types of solution are considered:

- modifications to existing designs, usually with limited effectiveness but at low cost and with possible short time to market;
- specific design of the rotorcraft and its components, possibly with high effectiveness but potentially higher cost and longer time to market.

A typical cure of the problem consists of interrupting the adverse feedback loop by 'disconnecting' the pilot. This is what happens when the pilot releases the controls, or simply softens the hold. This solution is trivial, and applies directly to the core of the problem. Unfortunately, it cannot be used in many relevant cases, in which releasing the controls would at best result in failing to fulfil a Mission Task Element (MTE), but could even result in fatal consequences.

Another approach consists of 'disconnecting' the pilot in the precise range of frequencies that characterises the adverse coupling, by applying a notch filter, i.e. a filter of the form

$$H_{\text{notch}} = \frac{s^2 + 2\frac{d}{c}\omega_0 s + \omega_0^2}{s^2 + 2\frac{1}{c}\omega_0 s + \omega_0^2} \tag{9}$$

that cancels the undesired couple of poles of frequency ω_0 and replaces them with another couple with the same frequency but higher damping ratio, as illustrated in Figure 16 with respect to the mesomorphic pilot transfer function of Eq. (2). The effect of applying the notch filter of Eq. (9) between the pilot's output and the input to the control system actuators is illustrated in Figure 17. This operation is common practise in augmented aircraft, but in principle it could be applied as well to vehicles with minimal or null augmentation, by designing the mechanics of the control system in order to behave as a mechanical equivalent to a notch filter. In this case, the pilot is still excited by the airframe, and this excitation results in an unintended feeding of adverse inputs in the controls. However those adverse signals are almost cancelled, or at least attenuated by the filter. This solution is not trivial because it is impractical without significant augmentation. Also, it requires careful tuning of the filter with respect to a frequency that typically depends on the rotorcraft and pilot configuration, and may also depend on the flight condition.

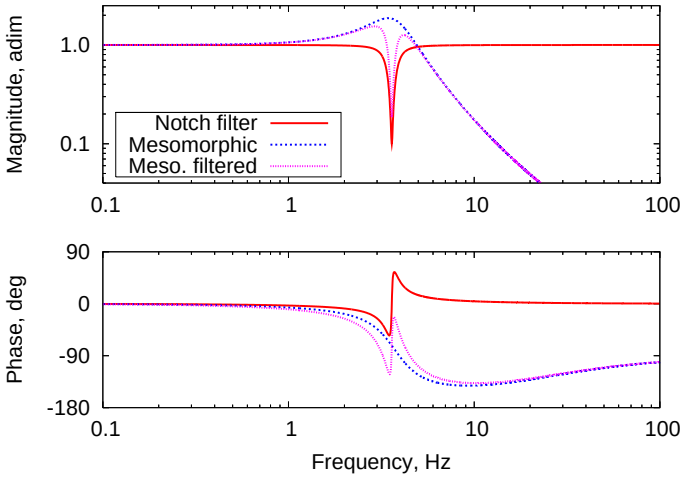

Figure 16: Application of a notch filter to the mesomorphic pilot transfer function of Eq. (2).

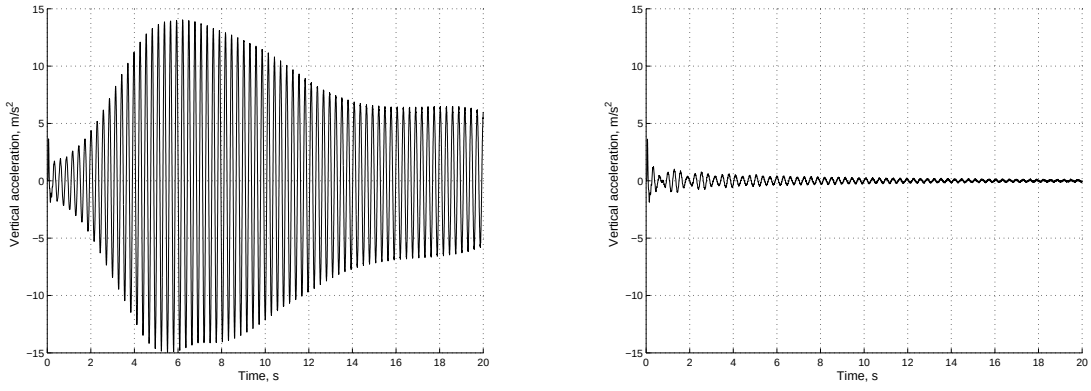

Figure 17: Vertical acceleration of the airframe, controlled by a mesomorphic co-pilot, after a disturbance. Reference case (left); with the notch filter of Eq. (9) (right).

Promising improvements are foreseen when a complete redesign of the cockpit layout is possible. The vertical bouncing phenomenon could be alleviated, for example, by replacing the conventional control stick with a sidestick or with a thrust control level, typical solutions for fixed wing aircraft.

The capability to predict the origin of adverse interactions at the conceptual and preliminary design phases would allow to consider airframe and cockpit layout design solutions that naturally decouple the airframe dynamics and the pilot, for example by attaching the pilot's seat and the controls in correspondence to modal nodes.

Finally, the availability of high or full authority FCS would allow the efficient filtering of undesired, adverse couplings with the pilot. However, it is important to realise that the design and tuning of those FCS may represent a formidable task. The availability of detailed, accurate and effective models is instrumental for the successful design of FCS.

Concluding Remarks

This paper presented the current status and recent achievements of the GARTEUR HC AG-16 on aeroelastic rotorcraft-pilot coupling (RPC). The activity focused on determining the aeroservoelastic modelling capabilities required to predict the complex interactional phenomena at the root of the unintended amplification of oscillations occurring in rotorcraft in the range of frequencies comprised between 2 and 8 Hz. Different approaches to the aeroelastic analysis of rotorcraft have been used by three partners of the project. Focus has been put on the aeroservoelastic simulation of the BO105 helicopter, coupled to transfer function based models of the pilot's passive impedance. Passive pilot transfer functions available from the literature have been complemented by similar models identified from specific measurements performed during a dedicated experimental campaign. The pilot modelling activity will proceed with the identification of the biomechanical properties required to set up a parametric multibody model of the pilot's arm. This model will possibly allow to compute pilot transfer functions for generic reference conditions and cockpit layouts. The work presented in this paper provided an initial assessment of the modelling capabilities required to address the coupled rotorcraft-pilot problem from an aeroservoelastic point of view. The activity is far from complete, and the issue of determining useful guidelines for RPC-free rotorcraft is not solved yet. Further development would probably come from a deeper analysis of many of the aspects that have been little more than outlined in this paper.

References

[1] "GARTEUR HC AG-16: Rigid body and aeroelastic rotorcraft-pilot coupling — prediction tools and means of prevention." `http://www.garteur.org/`.

[2] O. Dieterich, J. Götz, B. DangVu, H. Haverdings, P. Masarati, M. Pavel, M. Jump, and M. Gennaretti, "Adverse rotorcraft-pilot coupling: Recent research activities in Europe," in *34th European Rotorcraft Forum*, (Liverpool, UK), September 16–19 2008.

[3] M. Jump, S. Hodge, B. DangVu, P. Masarati, G. Quaranta, M. Mattaboni, M. Pavel, and O. Dieterich, "Adverse rotorcraft-pilot coupling: The construction of the test campaigns at the University of Liverpool," in *34th European Rotorcraft Forum*, (Liverpool, UK), September 16–19 2008.

[4] M. Pavel, B. DangVu, J. Götz, M. Jump, O. Dieterich, and H. Haverdings, "Adverse rotorcraft-pilot coupling: Prediction and suppression of rigid body RPC," in *34th European Rotorcraft Forum*, (Liverpool, UK), September 16–19 2008.

[5] R. B. Walden, "A retrospective survey of pilot-structural coupling instabilities in naval rotorcraft," in *63rd Annual Forum of the American Helicopter Society*, (Virginia Beach, VA), May 1–3 2007.

[6] M. Griffin, *Handbook of Human Vibration*. London: Academic Press, 1990.

[7] D. McRuer, "Pilot–induced oscillations and human dynamic behavior," CR 4683, NASA, 1995.

[8] J. R. Mayo, "The involuntary participation of a human pilot in a helicopter collective control loop," in 15^{th} *European Rotorcraft Forum*, (Amsterdam, The Netherlands), pp. 81.1–12, 12–15 September 1989.

[9] W. Johnson, "Technology drivers in the development of CAMRAD II," in *American Helicopter Society Aeromechanics Specialists Conference*, (San Francisco, California), January 19–21 1994.

[10] "MBDyn: Multibody Dynamics." `http://www.aero.polimi.it/~mbdyn/`.

[11] G. Quaranta, P. Masarati, and P. Mantegazza, "Assessing the local stability of periodic motions for large multibody nonlinear systems using POD," *Journal of Sound and Vibration*, vol. 271, no. 3–5, pp. 1015–1038, 2004.

[12] D. Hodges and E. Dowell, "Nonlinear equation for the elastic bending and torsion of twisted nonuniform rotor blades," TN D-7818, NASA, 1974.

[13] J. M. Greenberg, "Airfoil in sinusoidal motion in a pulsating stream," TN 1326, NACA, 1947.

[14] M. Gennaretti and G. Bernardini, "Novel boundary integral formulation for blade-vortex interaction aerodynamics of helicopter rotors," *AIAA Journal*, vol. 45, no. 6, pp. 1169–1176, 2007.

[15] T. C. Parham, D. Popelka, D. G. Miller, and A. T. Froebel, "V–22 pilot-in-the-loop aeroelastic stability analysis," in *AHS 47th Annual Forum*, (Phoenix, AZ), May 1991.

[16] T. Parham Jr. and L. M. Corso, "Aeroelastic and aeroservoelastic stability of the BA 609," in *25th European Rotorcraft Forum*, (Rome, Italy), September 14–16 1999.

[17] M. Mattaboni, A. Fumagalli, M. Jump, P. Masarati, and G. Quaranta, "Biomechanical pilot properties identification by inverse kinematics/inverse dynamics multibody analysis," in *ICAS-International Council for the Aeronautical Sciences*, (Anchorage, Alaska, USA), September 14–19 2008.

[18] T. Theodorsen, "General theory of aerodynamic instability and the mechanism of flutter," Report 496, NACA, 1935.